Macromolecules

Article

pubs.acs.org/Macromolecules

# Low-Temperature Processable Degradable Polyesters

Ikuo Taniguchi*,† and Nathan G. Lovell‡

†Chemical Research Group, Research Institute of Innovative Technology for the Earth, 9-2 Kizugawadai, Kizugawa, Kyoto 619-0292, Japan

‡Department of Materials Sciences and Engineering, Massachusetts Institute of Technology, 77 Massachusetts Avenue, Cambridge, Massachusetts 02139, United States

Supporting Information

**ABSTRACT:** Block copolymers composed of a low-$T_g$ and high-$T_g$ block, with suitable pressure miscibility characteristics, can be formed at low temperature through the application of pressure. Aliphatic block copolyesters composed of poly(ε-caprolactone) derivatives and poly(L-lactide) show room temperature processability under hydraulic pressure of 34.5 MPa without polymer degradation. The mechanism of the pressure-induced flow is investigated by small-angle X-ray scattering. A scattering associated with a lamellae structure observed at ambient conditions decreases with elevating hydrostatic pressures, indicating pressure-induced phase mixing. Traces of the pressure-induced phase transition are studied by differential scanning calorimetry and X-ray diffraction. Tensile test of the block copolymers reveals that the mechanical properties can be readily controlled by changing composition, molecular weight, and chemical structure of the blocks. Among them, the hard segment PLLA fraction is the key factor to characterize the properties. Young's modulus of the block copolyesters is similar to that of polyethylene.

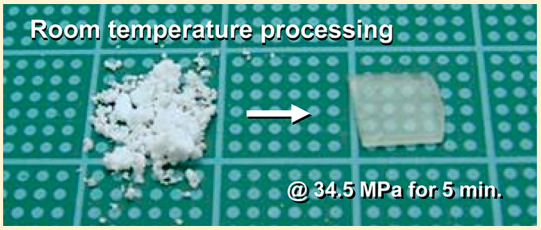


Downloaded via PURDUE UNIV on December 26, 2025 at 02:11:50 (UTC).
See https://pubs.acs.org/sharingguidelines for options on how to legitimately share published articles.

## INTRODUCTION

Since the mid-1970s, there has been growing interest in use of degradable polymers as alternatives to common nondegradable polymers derived from fossil resources, and various degradable polymers have been developed.[1−5] Among them, aliphatic polyesters, such as poly(ε-caprolactone) (PCL), poly(L-lactide) (PLLA), and poly(glycolic acid), have been extensively studied due to their synthetic feasibility and well-defined chemistry.[6,7] However, those aliphatic polyesters have several impediments to practical use. In particular, these materials suffer from poor thermal properties. Several approaches have been taken to produce greater thermoresistance through incorporation of aromatic components. These approaches, however, result in decreased degradability and require high-temperature molding processes, leading to higher energy consumption.[8−11] In addition, the thermal degradation temperatures of those polyesters are usually close to the melting temperatures, limiting the melt-processability and recycling.[12,13]

As a potential solution to this problem, Gonzalez-Leon and co-workers have conducted theoretical investigations into plastics termed "baroplastics" that can be processed at low temperatures through pressure-induced flow.[14−16] They developed several baroplastic block copolymer and core−shell nanoparticle systems, including polystyrene/poly(*n*-alkyl acrylates). Each of these materials is composed of a low-$T_g$ (glass transition temperature) soft component and a high-$T_g$ hard component. Under ambient pressure, the polymer blocks are immiscible and phase separate, leading to a material with good mechanical properties. Under elevated pressure, the two phases become miscible, leading to flow. This method uses pressure, rather than temperature, to induce flow, resulting in materials that can be processed at temperatures as low as room temperature. These polymeric systems may be designed using the compressible regular solution model (CRS),[17] an extension of the Flory−Huggins regular solution model for polymer mixtures that incorporates compressible segments. For binary compressible polymer blends, the free energy change of mixing per unit volume is expressed as eq 1:

$$\Delta g_{mix} = kT\left(\frac{\phi_A\tilde{\rho}_A}{N_A\nu_A}\ln\phi_A + \frac{\phi_B\tilde{\rho}_B}{N_B\nu_B}\ln\phi_B\right) + \phi_A\phi_B\tilde{\rho}_A\tilde{\rho}_B(\delta_{A,0}-\delta_{B,0})^2 + \phi_A\phi_B(\tilde{\rho}_A-\tilde{\rho}_B)(\delta_A{}^2-\delta_B{}^2) \quad (1)$$

Here, $k$ is the Boltzmann constant; $\phi_i$, $N_i$, and $\nu_i$ are the volume fraction, number of segments per chain, and hard core segmental volume of the $i$th component. $\delta_{i,0}$ and $\delta_i$ are the solubility parameters at temperatures 0 K and temperature $T$, respectively. $\tilde{\rho}_i$ is the reduced density, and $\rho_i$ is the density at temperature $T$. $\tilde{\rho}_i = \rho_i/\rho_i^*$, where $\rho_i^*$ is the hard core density (0 K) defined as $\rho_i^* = M_{u,i}/N_0\nu_i$ ($M_{u,i}$: the monomer molecular mass; $N_0$: Avogadro's number). In this equation, the third term arises from compressibility while the first two terms are analogous to the Flory−Huggins entropy and enthalpy of mixing terms. Equation 1 can be used to predict phase diagrams solely from pure component properties and has successfully

Received: June 17, 2012
Revised: August 19, 2012
Published: September 14, 2012

 © 2012 American Chemical Society 

captured the qualitative phase behavior of over 30 weakly interacting polymer pairs.[17−19]

In the present study, we extend this idea to develop pressure-processable degradable polymeric materials, namely aliphatic block copolyester systems. The pressure-induced flow of these systems is facilitated by pressure-enhanced miscibility of the soft and hard components. Candidate polymer pairs expected to exhibit the desired thermodynamic behavior were chosen based on free energy calculations using eq 1. Three degradable block copolymers were designed and synthesized by two-step ring-opening polymerization of lactones and lactide. The low-temperature processing and mechanical properties of these block copolyesters were investigated.

## EXPERIMENTAL SECTION

**Materials.** 1,4-Cyclohexanedione monoethylene acetal (Alfa Aesar, Ward Hill, MA), 3-chloroperoxybenzoic acid (ca. 70%, Aldrich, WI), tetrahydro-4*H*-pyran-4-one (Aldrich), stannous octate ($SnOct_2$, Alfa Aesar), and anhydrous toluene (Aldrich) were used as received. L-Lactide (L-LA, Aldrich) was twice purified by recrystallization in dry toluene and dried under reduced pressure ($10^{-2}$ mmHg) for at least 12 h before use. ε-Caprolactone (ε-CL, Aldrich) was dried over calcium hydride for 48 h at room temperature and distilled under reduced pressure right before use. Aluminum isopropoxide ($Al(O^iPr)_3$, Aldrich) was twice distilled under reduced pressure and then dissolved in dry toluene under nitrogen. $Al(O^iPr)_3$ concentration was determined from the degree of polymerization of PCL in ring-opening polymerization of ε-CL with this catalyst. Ethanol (Alfa Aesar) was dried over 3 Å molecular sieves. Other organic and inorganic compounds were of reagent grade and used without further purification.

**Synthesis of Lactone Monomers.** DXO (1,5-Dioxepan-2-one) was synthesized by Baeyer−Villiger oxidation of tetrahydro-4*H*-pyran-4-one acetal by Albertsson and co-workers.[20,21] TOSUO (1,4,8-trioxa[4,6]spiro-9-undecanone) was also derived by Baeyer−Villiger oxidation from 1,4-cyclohexanedione monoethylene acetal following the methods reported by Jérôme and co-workers.[22−24] The details of the syntheses and purifications are described in the Supporting Information.

**Synthesis of Poly(ε-caprolactone)-*b*-poly(L-lactide) (PCL-*b*-PLLA).** PCL-*b*-PLLA was synthesized by two-step ring-opening polymerization of ε-CL and L-LA. $SnOct_2$ (80 mg, 0.2 mmol) and ethanol (70 mg, 1.5 mmol) were added to a flame-dried round-bottom flask equipped with a magnetic stir bar, under an inert atmosphere in a glovebox (Unilab (1200/780), Mbraun, Stratham, NH). ε-CL (11,4 g, 100 mmol) and 5 mL of dry toluene were successively added to the flask through a rubber septum with syringes. The reaction mixture was stirred at 110 °C for 24 h, when the absence of ε-CL monomer was found by $^1$H NMR. L-LA (10.2 g, 71 mmol) was then added to the reaction flask in a glovebox. The mixture was kept at 110 °C for a week. After block copolymerization, dichloromethane was added to dissolve the polymer, which was recovered by reprecipitation in methanol containing excess 1 N HCl.

**Synthesis of Poly(1,5-dioxepan-2-one)-*b*-poly(L-lactide) (PDXO-*b*-PLLA).** A typical synthesis was performed as follows: $SnOct_2$ (40 mg, 0.1 mmol) and ethanol (8 mg, 0.2 mmol) were added to a flame-dried round-bottom flask equipped with a magnetic stir bar, under an inert atmosphere in a glovebox. DXO (4.7 g, 40 mmol) and dry toluene (5 mL) were added successively to the flask through a rubber septum with syringes. Subsequent second step ring-opening polymerization and purification were the same as described above. L-LA (7 g, 49 mmol) was added for block copolymer synthesis.

**Synthesis of Poly(ε-caprolactone-*r*-5 ethylene ketal ε-caprolactone)-*b*-poly(L-lactide) (PmCL-*b*-PLLA).** A typical synthesis of high molecular weight PmCL-*b*-PLLA was as follows: TOSUO (2.5 g, 15 mmol), $SnOct_2$ (40 mg, 0.1 mmol), and ethanol (8 mg, 0.2 mmol) were added to a flame-dried round-bottom flask equipped with a magnetic stir bar under an inert atmosphere in a glovebox. ε-CL (7.2 g, 63 mmol) and 5 mL of dry toluene were successively added into the flask through a rubber septum with syringes. Subsequent second step ring-opening polymerization and purification were the same as described above. L-LA (8.0 g, 56 mmol) was used for block copolymer synthesis. On the other hand, low molecular weight PmCL-*b*-PLLA was synthesized using $Al(O^iPr)_3$. In brief, TOSUO was added to a flame-dried round-bottom flask equipped with a magnetic stirring bar under an inert atmosphere in a glovebox. ε-CL, dry toluene, and initiator $Al(O^iPr)_3$−toluene solution were successively added to the flask through a rubber septum with syringes. Total monomer and initiator (ethanol) concentrations were kept to 1 M and 13 mM, respectively. After 15 h at 25 °C, CL monomer was not found in $^1$H NMR, and a specified amount of L-LA was added in a glovebox. The reaction mixture was kept at 80 °C for 72 h. The resulting polymers were recovered by reprecipitation in cold methanol containing excess 1 N HCl.

**Processing of Block Copolymers.** Each block copolymer was processed by compression molding using a hydraulic pressure of 34.5 MPa (5000 psi) for 5 min with a Grimco hydraulic press (Grimco, NJ). The processing temperature for PDXO-*b*-PLLA and PmCL-*b*-PLLA was 25 °C, while PCL-*b*-PLLA was pressed at 65 °C for 5 min.

**Measurements.** $^1$H and $^{13}$C NMR spectra were recorded in $CDCl_3$ at 25 °C using a Bruker AM400 apparatus operating at 400 and 100 MHz, respectively. Differential scanning calorimetry (DSC) was performed with a TA Q-100 (TA Instruments, New Castle, DE). Transition temperatures, $T_g$ and $T_m$ (melting temperature), were measured after cooling the sample to −100 °C followed by heating to 190 °C at a heating rate of 10 °C/min. For the measurement of heat of crystallization ($\Delta H_c$) and heat of fusion ($\Delta H_m$), the sample was heated at 2 °C/min. X-ray diffraction (XRD) was carried out with a Rigaku RU300 X-ray diffractometer (camera length: 185 mm) (Rigaku, Tokyo, Japan) with a Cu K$\alpha$ X-ray ($\lambda$: 1.5418 Å). Each sample was scanned from 5° to 40° in 2$\theta$ at 1 deg/min and at intervals of 0.02 deg. Small-angle X-ray scattering (SAXS) measurements were performed on a Rigaku Nano-Viewer (Rigaku) consisting of a Cu K$\alpha$ X-ray source, 3 pinhole-collimated beam, and a Pilatus 100 K 2D detector (Dectris, Baden, Switzerland). The camera length and exposure time were 1253 mm and 10 min, respectively. A pressure cell having diamond windows (Syn Corporation, Kyoto, Japan) was used to measure the effects of pressure *in situ* on PmCL-*b*-PLLA using dry nitrogen as a pressurizing medium at 35 °C. Scattering data were collected for 10 min at each pressure during both an upward and downward pressure sweep. Mechanical properties of the block copolymers were measured using a 8848 Micro Tester (Instron, Norwood, MA) with displacement rates of 0.25 and 0.5 mm/s (strain rates between 0.6 and 1.4%/s) to find Young's modulus and strain-to-break. Mechanical testing samples were processed from powder into a flat sheet 0.4−1.1 mm thick. Following processing, samples were cut using a custom dogbone-shaped specimen cutter 1.87 to 2.25 mm wide and ∼45 mm long. Commercial PCL ($M_n$: 80 kDa, Aldrich) and PLLA ($M_n$: 85−160 kDa, Aldrich) were processed and tested in the same fashion, but at processing temperatures of 65 and 190 °C, respectively. Size exclusion chromatography (SEC) system consisted of a Viscotek GPCmax VE2001 (Viscotek, TX) and a Viscotek VE 3580 RI detector (Viscotek). Styragel HR4 gel columns of T92881B 12, W21721G 024, and T53311A 08 ($\phi$ 7.8 × 300 mm, Waters, Milford, MA) in series were used. Tetrahydrofuran was used as an eluent at a flow rate of 1.0 mL/min and at 25 °C. The molecular weight was calibrated with polystyrene standards (Aldrich).

## RESULTS AND DISCUSSION

In designing low-temperature processable degradable polyesters, the idea of "baroplasticity" or pressure-induced flow has been applied. A binary system was chosen in this study, and candidate polymer pairs were investigated to fulfill several requirements described below.

**Prediction of Polymer Pairs.** Pollard and co-workers first reported that the miscibility of poly(*n*-butyl methacrylate)-*b*-polystyrene was enhanced by the application of pressure, as


dx.doi.org/10.1021/ma301230y | Macromolecules 2012, 45, 7420−7428

observed by small-angle neutron scattering (SANS).[25] Follow-up studies found similar phase behavior for various block copolymers of polystyrene and other poly(*n*-alkyl methacrylate) species.[14−16,18,19,26] For a two-component system, these extensive investigations revealed several key factors for production of room-temperature processable polymers: (1) A two-component system must show an upper disorder-to-order transition (UDOT) wherein two chemically distinct polymer chains covalently bonded together undergo a order-to-disorder transition upon heating. A plausible pressure-induced phase transition is represented in Figure 1. When a binary system has

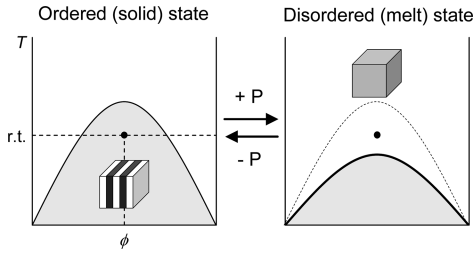


**Figure 1.** Pressure-induced phase transition of copolymers with UDOT phase diagram.

symmetrical weight fraction as designated point at ambient temperature in Figure 1, the system show phase-separated structure. The binodal curve can be pushed down when pressure is applied. In that case, the designated point places above the binodal line under pressure, which means the system turns to be disordered or phase mixed state. The maximum temperature of the binodal curve under pressure must be below the decomposition temperature of the polymers. (2) The system should have a large interface between coexisting phases. This requirement arises because pressure-induced mixing takes place on the nanometer length scale near the interface.[25] Consequently, microphase-separated structures are required to produce sufficient fluidity to be processed under applied pressure. (3) The $T_g$s of a polymer pair should be significantly above or below ambient temperature, and the low-$T_g$ soft block should be amorphous and flow at ambient temperature. (4) It was empirically found that the ambient densities of the two blocks should be similar ($0.94\tilde{\rho}_A < \tilde{\rho}_B < 1.06\tilde{\rho}_A$). (5) The third term of eq 1, $\phi_A\phi_B(\tilde{\rho}_A - \tilde{\rho}_B)(\delta_A{}^2 - \delta_B{}^2)$, approaches zero at 0 K from negative values. The CRS model has been a powerful tool to predict thermodynamic behavior of polymer blends and has been employed to design potential degradable polymer systems with low-temperature flow.

For such a polymer candidate with low-temperature formability, pairs of polymer segments in a block copolymer should have a low-$T_g$ amorphous and a high-$T_g$ semicrystalline component. Under pressure, both components can be miscible, and the resulting mixture shows flow nature at the temperature. Although a number of degradable polyesters have been prepared, only a few examples have been reported, which can serve as candidates for the soft component: PDXO (poly(1,5-dioxepan-2-one) reported by Albertsson and co-workers,[20,21] and PmCL (poly(ε-caprolactone-*r*-5 ethylene ketal ε-caprolactone)) by Jérôme and co-workers.[22−24] The $T_g$ of PDXO is −38 °C while that of PmCL varies from −60 to −40 °C depending on the copolymerization ratio between ε-CL and TOSUO. PmCL is completely amorphous when incorporated with greater than 15 mol % TOSUO[23] and has the potential for further modification through transformation of the ketal to carbonyl and hydroxyl groups[22] or grafting aminooxy compounds by a chemoselective approach.[27] For the hard component, we chose PLLA due to its excellent mechanical properties and degradability. Phase diagrams for each material were calculated with the CRS model from pure group contribution parameters.[28] The pure component properties, $\tilde{\rho}_i$ and $\delta^2$, were determined from group contribution calculations. $\rho(T)$ was obtained from the thermal expansion coefficient $\alpha$ and hard core density $\rho^*$ or volume $\nu$, which was the segmental volume extrapolated to 0 K with the melt-state thermal expansion coefficient by the relation $\rho(T) = \rho^* \exp(-\alpha T)$.[29] The cohesive energy density ($\delta^2(T)$) was also obtained by the relation $\delta^2(T) = \delta^2(298)(\tilde{\rho}_i(T)/\tilde{\rho}_i(298))$, where $\tilde{\rho}_i(298)$ was the room temperature cohesive energy density calculated according to van Krevelen.[30] The thermodynamic parameters used in phase diagram prediction are listed in Table S1. The phase behaviors of three polymer pairs predicted by the CRS model are illustrated in Figure 2. The UDOTs for PDXO/

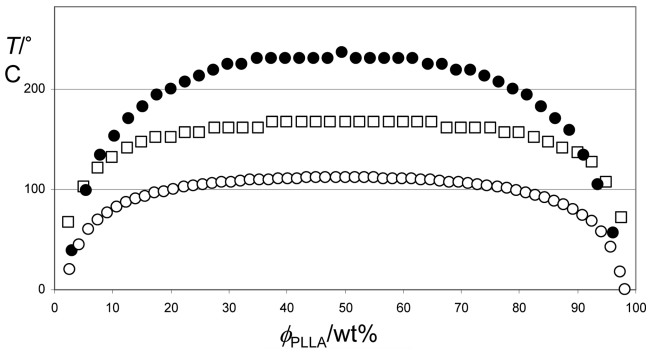


**Figure 2.** Predicted phase diagrams of PDXO/PLLA (open square), PmCL/PLLA (open circle), and PCL/PLLA (filled circle). Total molecular weight of the block copolymer is 100 kDa, and the weight fraction of each block is 50 wt %.

PLLA, PmCL/PLLA, and PCL/PLLA systems were plotted based on pure group contribution parameters. Of the candidate systems calculated, the most miscible was predicted to be PDXO/PLLA system, while the least was PCL/PLLA system.

**Block Copolymer Syntheses and Basic Thermal Properties.** Degradable block copolymers have been synthesized by two-step ring-opening polymerization of lactones and lactide as shown in Scheme 1. Polymerization was initiated with $Al(O^iPr)_3$[31] for low molecular weight PmCL-*b*-PLA and $SnOct_2$[32−34] for high molecular weight block copolymers.

**Scheme 1. Synthetic Route of Degradable Block Copolyester by Two-Step Ring-Opening Polymerization**

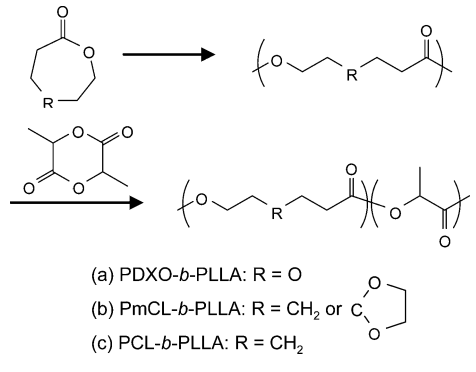



dx.doi.org/10.1021/ma301230y | *Macromolecules* 2012, 45, 7420−7428

**Table 1. Results of Ring-Opening Polymerization and Thermal Properties of Prepared Block Copolyesters**

| | | | feed/mmol | | | | | | | | | |
|---|---|---|---|---|---|---|---|---|---|---|---|---|
| | | | lactone | | | | | | | | | |
| run | copolymer | catalyst | ε-CL | TOSUO | DXO | L-LA | lactone:initiator:catalyst | PLLA[a]/wt % | $10^{-3}M_w$[b] | $M_w/M_n$[b] | $T_g$[c]/°C | $T_m$[c]/°C |
| 1 | PmCL-*b*-PLLA | $Al(O^iPr)_3$ | 53 | 17 | | 63 | 78:1.2:1.0 | 43 | 13 | 1.3 | −54 | 159 |
| 2 | PmCL-*b*-PLLA | $Al(O^iPr)_3$ | 53 | 17 | | 49 | 78:1.2:1.0 | 36 | 15 | 1.2 | −52 | 161 |
| 3 | PmCL-*b*-PLLA | $Al(O^iPr)_3$ | 44 | 15 | | 41 | 59:1.0:0.8 | 41 | 16 | 1.3 | −54 | 163 |
| 4 | PmCL-*b*-PLLA | $Al(O^iPr)_3$ | 4 | 14 | | 69 | 58:1.0:0.8 | 52 | 20 | 1.3 | −52 | 168 |
| 5 | PmCL-*b*-PLLA | $Al(O^iPr)_3$ | 35 | 12 | | 28 | 47:0.8:0.6 | 13 | 11 | 1.2 | −52 | n.d. |
| 6 | PmCL-*b*-PLLA | $Al(O^iPr)_3$ | 70 | 17 | | 69 | 87:1.4:1.1 | 31 | 14 | 1.2 | −52 | n.d. |
| 7 | PmCL-*b*-PLLA | $SnOct_2$ | 61 | 31 | | 90 | 92:0.6:0.3 | 48 | 66 | 1.5 | −48 | 163 |
| 8 | PmCL-*b*-PLLA | $SnOct_2$ | 63 | 15 | | 69 | 78:0.2:0.3 | 49 | 158 | 1.8 | −58 | 173 |
| 9 | PmCL-*b*-PLLA | $SnOct_2$ | 58 | 17 | | 118 | 75:0.2:0.3 | 60 | 186 | 1.7 | −53 | 171 |
| 10 | PDXO-*b*-PLLA | $SnOct_2$ | | | 65 | 49 | 65:0.2:0.1 | 53 | 184 | 1.5 | −36 | 172 |
| 11 | PDXO-*b*-PLLA | $SnOct_2$ | | | 45 | 49 | 45:0.2:0.1 | 61 | 126 | 1.4 | −32 | 172 |
| 12 | PCL-*b*-PLLA | $SnOct_2$ | 100 | | | 71 | 100:1.2:0.3 | 44 | 203 | 1.3 | −60 | 58172 |

[a]LA content (wt %) was determined by $^1$H NMR. [b]Molecular weight and polydispersity index were determined by SEC. [c]$T_g$ of soft block and $T_m$ of hard block were determined by DSC at a heating rate of 10 °C/min.

Molecular weights and transition temperatures ($T_g$ and $T_m$) were determined by SEC and DSC, respectively, as summarized in Table 1. With $SnOct_2$, the polymerization was conducted to suppress transesterification at 110 °C.[35] Formation of the block copolyesters was indicated by $^{13}$C NMR as shown in Figure 3.

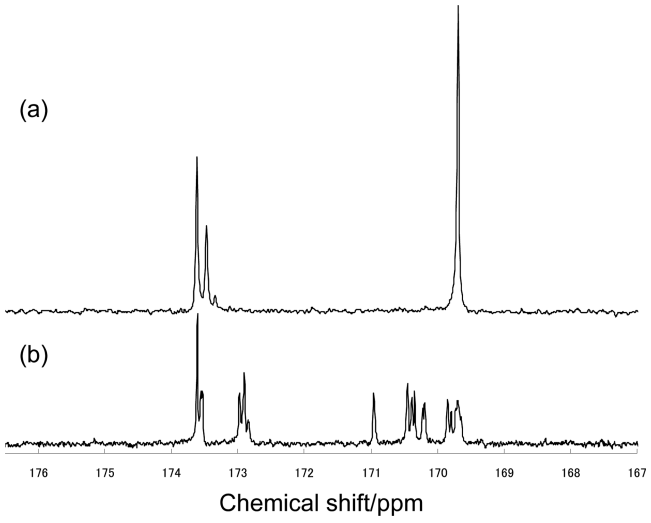


**Figure 3.** Carbonyl region of $^{13}$C NMR spectra of polyesters obtained by (a) two-step ring-opening polymerization of (ε-CL + TOSUO) and LLA and by (b) simultaneous ring-opening copolymerization of ε-CL and L-LA in $CDCl_3$ at 298 K.

The carbonyl region signal of polyesters in $^{13}$C NMR is sensitive to the sequence effects.[36] For example, with PmCL/PLLA copolymer prepared by two-step ring-opening polymerization (Figure 3a), peaks at 173.4 and 173.6 ppm correspond to the presence of blocky structures of TOSUO and ε-CL, respectively, while a signal between the two peaks at 173.5 ppm indicated random sequence of TOSUO and ε-CL. On the other hand, after the second step ring-opening polymerization of L-lactide (L-LA), the absence of signals between 169.7 (PLLA block) and 173.4 ppm was explained by the formation of PmCL and PLLA blocks. Figure 3b exhibits the $^{13}$C NMR spectrum of copolyester obtained by simultaneous ring-opening copolymerization of ε-CL and L-LA. Random monomer sequence was suggested by the presence of multiple peaks between 173.6 and 169.7 ppm. $^1$H and $^{13}$C NMR spectra of the copolyesters are exhibited in Figures S1 and S2.

The $T_g$s of soft components PDXO and PmCL were −36 to −32 °C and −58 to −48 °C, respectively. The $T_g$ of PmCL was found to vary with the copolymerization ratio of ε-CL and TOSUO, while the $T_g$ of PCL homopolymer was −60 °C. The $T_m$s observed for the PLLA crystal were from 159 to 173 °C depending on the block length, and PCL-*b*-PLLA shows an additional $T_m$ from crystalline PCL at 58 °C (see Figure S3). Typical transition temperatures of each block found on DSC also supports formation of the block sequences. The PLLA content in the block copolymer can be readily tuned, and various copolyesters with PLLA fractions of 13−61 wt % were developed. When the PLLA fraction was below 40 wt %, PLLA cannot crystallize, and the resulting copolymers flow at ambient condition. Hard segment fraction between 40 and 60 wt % will be thus preferable for low-temperature formability based on the predicted phase diagram in Figure 2.

**Low-Temperature Processing.** The processability of degradable block copolyesters was examined by compression-molding using a standard hydraulic press at 34.5 MPa for 5 min. A typical example is shown in Figure 4. When the hard segment fraction was between 40 and 60 wt %, PDXO-*b*-PLLA and PmCL-*b*-PLLA polymers could be processed at 25 °C through the application of pressure, in spite of their high-$T_g$ PLLA component. The resulting molded objects were transparent. The room temperature processability of these materials suggests that the block copolyesters would flow under such

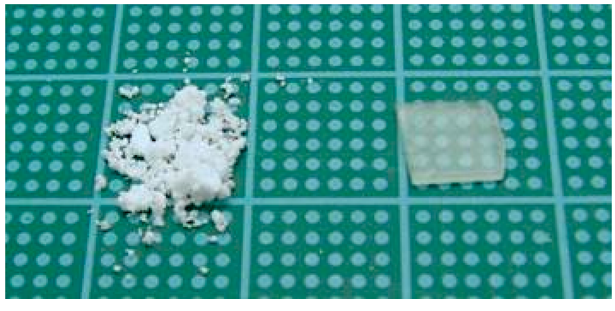

**Figure 4.** PmCL-*b*-PLLA ($M_w$: 60 kDa, LA: 50 wt %) before (left) and after (right) processing under 34.5 MPa for 5 min at 25 °C.


dx.doi.org/10.1021/ma301230y | Macromolecules 2012, 45, 7420−7428

Table 2. Change in $X_c$ of Block Copolymers before and after Processing Determined from DSC and XRD and $g$ Factors of Block Copolymers before and after Processing Determined from XRD[a]

| | | $X_c$/% by DSC | | $X_c$/% by XRD | | $g$ factor | |
|---|---|---|---|---|---|---|---|
| run | copolymer | before | after | before | after | before | after |
| 1 | PmCL-*b*-PLLA | 9.0 | 9.0 | 16.5 | 8.0 | n.t. | n.t. |
| 2 | PmCL-*b*-PLLA | 6.8 | 6.9 | 12.6 | 4.8 | n.t. | n.t. |
| 3 | PmCL-*b*-PLLA | 8.5 | 8.9 | 13.1 | 6.5 | n.t. | n.t. |
| 4 | PmCL-*b*-PLLA | 14.0 | 14.8 | 15.0 | 6.3 | n.t. | n.t. |
| 7 | PmCL-*b*-PLLA | 9.7 | 10.0 | 27.0 | 18.8 | 0.13 | 0.18 |
| 8 | PmCL-*b*-PLLA | 8.4 | 7.3 | 25.0 | 16.1 | 0.16 | 0.23 |
| 9 | PmCL-*b*-PLLA | 11.5 | 11.7 | 24.4 | 16.0 | 0.14 | 0.16 |
| 10 | PDXO-*b*-PLLA | 9.6 | 13.2 | 31.3 | 14.0 | 0.08 | 0.16 |
| 11 | PDXO-*b*-PLLA | 10.8 | 12.7 | 22.9 | 12.6 | n.t. | n.t. |
| 12 | PCL-*b*-PLLA | 16.1 (PCL), 6.4 (PLLA) | 12.9 (PCL), 6.4 (PLLA) | 38.1 (total) | 46.3 (total) | 0.12 | 0.29 |

[a]Processing conditions: 34.5 MPa for 5 min at 25 °C for PDXO-*b*-PLLA and PmCL-*b*-PLLA) or at 65 °C for PCL-*b*-PLLA. The $g$ factors were determined from the slope of Hosemann's plot (eq 3).

compression conditions. On the other hand, PCL-*b*-PLLA could not be processed at 25 °C due to PCL crystal. This polymer, however, could be processed at 65 °C higher than the $T_m$ of PCL crystal (58 °C), yet well below of the $T_m$ of PLLA. After processing, the molded polyester film was initially transparent but became opaque with time in a week. Heating at 80 °C can accelerate the crystallization of PCL, and the film turned opaque in a day. Molded PDXO-*b*-PLLAs and PmCL-*b*-PLLAs, by contrast, did not lose their transparency. This change in transparency results from crystallization of the PCL component under ambient conditions. The $T_g$ of the PCL block is −60 °C, and rearrangement of soft segment chains occurs at room temperature even though the chain flexibility is suppressed by PLLA hard segment.

**Change in Crystallinity.** The observed low-temperature processing indicates pressure-induced phase mixing at much lower temperatures than the melting point of PLLA. To investigate this pressure-induced phase transition, changes in degree of crystallinity ($X_c$) of PLLA before and after processing were studied by DSC and XRD. While copolymers obtained after reprecipitation were used as a "before processing" specimen, processed ("after processing") samples were prepared by compressing the before processing polymer powder at 34.5 MPa for 5 min at 25 °C. In the DSC measurement, the $X_c$ was calculated by the equation

$$X_c = (\Delta H_c + \Delta H_m)/\Delta H_{m,100\%} \times 100 \quad (2)$$

where $\Delta H_c$ and $\Delta H_m$ are heat of crystallization and fusion observed, respectively; $\Delta H_{m,100\%}$ is the heat of fusion of the complete crystal. The DSC thermograms of block copolyesters are presented in Figure S3, and the results are given in Table 2. The values of $\Delta H_{m,100\%}$ for PLLA and PCL employed are 135 and 142 J/g, respectively.[37] The $X_c$s of PLLA portion of both PDXO-*b*-PLLA and PmCL-*b*-PLLA increased in proportion to the PLLA contents. Regardless of molecular weight and PLLA content, the $X_c$ of the processed sample did not change much in comparison to that of the before processing sample. This indicates that further crystallization of PLLA did not proceed during pressure processing. The $X_c$ of PLLA even did not change after a month at ambient temperature. In contrast, with PCL-*b*-PLLA, both the PCL and PLLA blocks are crystalline, and crystallization of these blocks can be determined separately before and after processing. The $X_c$s of the PLLA block before and after processing were identical. The $X_c$ of PCL, however, decreased from 16.1 to 12.9% after compression molding. This suggests that a portion of the PCL block is kinetically prevented from crystallization for a brief period following pressure-induced mixing. The processed specimen became opaque with time at room temperature, as the PCL block gradually crystallizes.

The change in $X_c$ after processing was also studied by XRD in Table 2. The $X_c$ was determined from the ratio of crystalline and amorphous peaks. The scattering profiles are seen in Figure 5. With room temperature processable PDXO-*b*-PLLA and PmCL-*b*-PLLA, crystalline peaks typical of PLLA were observed at 16.7° ((200) and (110) Miller plains), 19.1° ((203) and (113)), and 22.3° ((210)). While the scattering angles of these peaks were identical, the intensities were decreased after processing, resulting in a decrease in the $X_c$ values of those block copolymers. However, the results obtained by XRD are inconsistent with those from DSC. One possible explanation is that the decrease in $X_c$ found by XRD may arise from a defect in the PLLA crystallite formed during processing which DSC may not count. This hypothesis may be tested through further examination of the XRD results, using the crystal parameters of PLLA. Hosemann derived an equation for relative evaluation of crystal defects using the $g$ factor of a paracrystal in eq 3:[38]

$$\delta b = (1/a)[(1/N) + p^2h^2g^2] \quad (3)$$

where $\delta\beta$, $a$, $N$, and $h$ are full width at half-maximum (fwhm) of a peak, the lattice size, the crystallite size, and a Miller index, respectively. As the first approximation, $a$-axis was employed for $h$. In this case, PLLA was taken as an $\alpha$-crystal based on the XRD pattern,[39] with an orthorhombic lattice structure having cell dimensions $a$ = 1.05, $b$ = 0.61, and $c$ = 2.88 nm.[40] By plotting $h^2$ for $\delta\beta$ of the three typical peaks of PLLA, the $g$ factor can be calculated from the slope as shown in Figure S4I. Results are summarized in Table 2. Although insufficient data were available to determine an accurate value, and some plots gave negative values at $y$-intercept due to the large crystallite size, the trends in change in degree of paracrystallinity and crystallite size can be interpreted. The addition of hydraulic pressure gave rise to $g$ factors in all cases plotted, which indicates that the degree of paracrystallinity increased after processing. In addition, the crystallite size also increased due to the decrease in $y$-intercept with the application of pressure. The Hosemann's plot suggests the formation of larger crystallites of PLLA with an increase in degree of paracrystallinity as a result of processing. These results suggest that defects in PLLA


dx.doi.org/10.1021/ma301230y | Macromolecules 2012, 45, 7420−7428

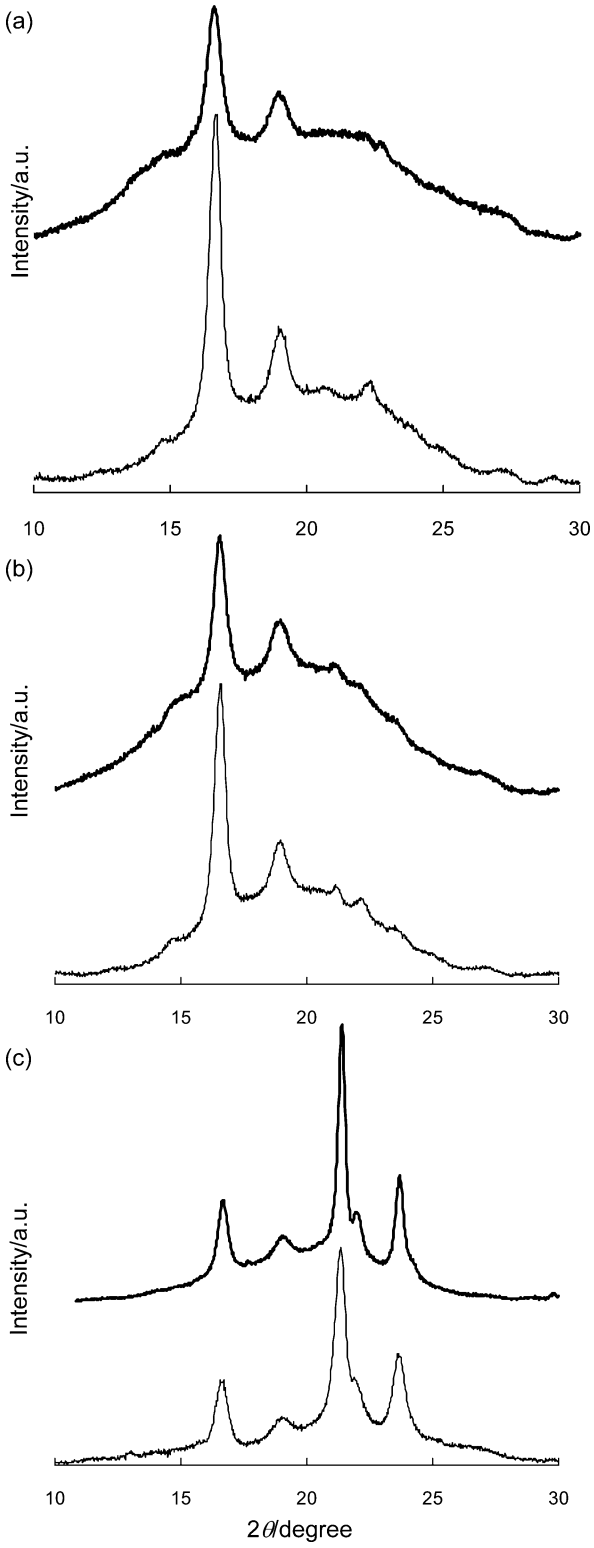


**Figure 5.** XRD spectra of (a) PDXO-*b*-PLLA ($M_w$: 126 kDa, LA: 61 wt %), (b) PmCL-*b*-PLLA ($M_w$: 158 kDa, LA: 49 wt %), and (c) PCL-*b*-PLLA ($M_w$: 203 kDa, LA: 44 wt %) before (plain line) and after (bold line) processing. The scan rate: 1 deg/min at intervals of 0.02 deg.

crystals formed as a consequence of processing could lead to a decrease in $X_c$ in PDXO-*b*-PLLAs and PmCL-*b*-PLLAs.

For PCL-*b*-PLLA incubated for a week at ambient temperature, determination of individual $X_c$s for PCL and PLLA was difficult because of overlapping the crystalline peaks. For these materials, only an overall $X_c$ can be calculated, which increased as a result of processing. The intensities of the peaks at 21.4° and 23.8°, corresponding to the PCL component ((110) and (200) Miller plains, respectively), increased by processing at 65 °C. Crystallization of the PCL component contributed to the increase in overall $X_c$ of PCL-*b*-PLLA.

The degradable block copolymers, PDXO-*b*-PLLA and PmCL-*b*-PLLA, show processability at ambient temperature while PCL-*b*-PLLA can only be processed above 65 °C, higher than the $T_m$ of PCL (at 58 °C). DSC revealed the $X_c$s of PDXO-*b*-PLLA and PmCL-*b*-PLLA were almost identical after processing. XRD provided more nuanced information, indicating that the crystal structure of PLLA changed by compression molding. The observed changes in crystallite size and degree of paracrystallinity in PLLA by processing can be explained by the following mechanism: through the application of a hydraulic pressure, each component of the block copolymers transfers from ordered (immiscible) state into the disordered (miscible) state, where the low-$T_g$ fluidized PDXO or PmCL partially solvate the high-$T_g$ PLLA. Upon removal of pressure, the disordered state immediately turns to ordered state, and soft segment may disturb the recrystallization of PLLA without defects at near the interface fused. As a result, an incomplete crystal will be formed. The observed changes in the degree of paracrystallinity provide further indications of pressure-induced phase transition through the application of pressure.

**Microphase Separation of Degradable Block Copolymers.** Block copolymers form microphase-separated structures upon phase transition depending on the compositions and molecular lengths of the blocks.[41] The phase-separated structures of the prepared degradable block copolymers were investigated by SAXS. Figure 6 shows representative scattering profiles of PmCL-*b*-PLLA ($M_W$: 60 kDa, LA: 50 wt %) under various pressures. At ambient pressure, a sharp peak was observed at $q_{max} = 3.13 \times 10^{-2}$ Å$^{-1}$. This peak can be attributed to a lamellar structure upon microphase separation. The average structural length $\Lambda_{ave}$ was 20.1 nm, as determined by eq 4:

$$\Lambda_{ave} = \frac{2\pi}{q_{max}} \quad (4)$$

Microphase-separated structures were also captured in the other block copolyesters, with $\Lambda_{ave}$ between 15 and 25 nm depending on the composition and block length of the degradable block copolyesters.

Microphase separation was further investigated by SAXS under various pressures to study the pressure-induced phase transition. At each applied pressure, the specimen was equilibrated for at least 2 h at 35 °C before collection of scattering profiles. In Figure 6, the peak intensities from the lamellar structure decreased gradually with elevating applied pressure from ambient to 75 MPa at 35 °C. The scattering intensity at 75 MPa decreased to about one-sixth of that at ambient pressure. In addition, $q_{max}$ and fwhm of the peak rose with increasing applied pressure. This means that phase mixing was observed with increasing pressure at this fixed temperature. Note, however, that this block copolyester could be processed at 30 MPa and 25 °C, indicating that it can be processed even while phase mixing is incomplete. On the basis of these results, we hypothesize that the hard PLLA phase is partially dissolved


dx.doi.org/10.1021/ma301230y | *Macromolecules* 2012, 45, 7420−7428

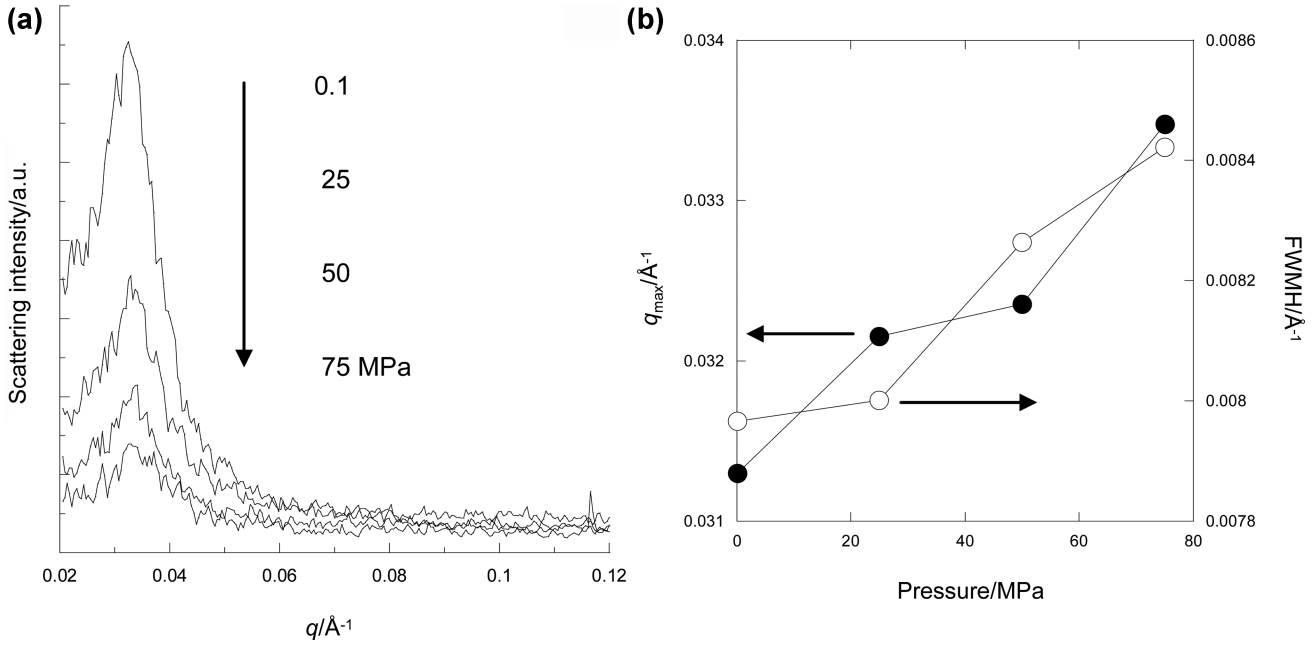


**Figure 6.** (a) SAXS spectra and (b) changes in $q_{max}$ and fwhm of the scattering peaks of PmCL-*b*-PLLA ($M_w$: 60 kDa, LA: 50 wt %) under various pressures at 35 °C.

**Table 3. Mechanical Properties of Various Degradable Block Copolyesters**[a]

| copolymers | $10^{-3}M_w$ | $M_w/M_n$ | LA/wt % | Young's modulus/MPa | strain-to-break/% | stress-at-break/MPa |
|---|---|---|---|---|---|---|
| PCL-*b*-PLLA | 170 | 1.7 | 55 | 950 ± 80 | 30 ± 20 | 38 ± 8 |
| PmCL-*b*-PLLA | 62 | 2.1 | 43 | 234 ± 8 | 36 ± 14 | 4.7 ± 0.2 |
| | 66 | 1.5 | 47 | 62 ± 20 | 22 ± 4 | 2.9 ± 1.0 |
| | 158 | 1.8 | 49 | 141 ± 22 | 14 ± 8 | 3.8 ± 0.3 |
| | 98 | 2.3 | 51 | 206 ± 13 | 16 ± 7 | 4.5 ± 1.0 |
| | 98 | 2.5 | 52 | 207 ± 26 | 17 ± 8 | 4.8 ± 0.7 |
| | 20 | 1.3 | 53 | 198 ± 27 | 11 ± 4 | 4.5 ± 0.8 |
| | 48 | 1.7 | 53 | 191 ± 12 | 7 ± 1 | 4.1 ± 1.3 |
| | 47 | 2.0 | 57 | 441 ± 10 | 4.8 ± 0.6 | 7.1 ± 0.4 |
| | 186 | 1.7 | 60 | 373 ± 45 | 2.0 ± 0.4 | 6.4 ± 0.2 |
| PDXO-*b*-PLLA | 98 | 1.9 | 40 | 26 ± 2 | 150 | 2.6 ± 0.3 |
| | 107 | 2.1 | 52 | 104 ± 2 | 18 | 5.1 ± 0.7 |
| | 184 | 1.5 | 53 | 204 ± 18 | 70 ± 12 | 7.8 ± 0.6 |
| | 126 | 1.4 | 61 | 459 ± 100 | n.d. | 10.3 ± 2.2 |
| PLLA | 80 | | 100 | 2670 | 1.5 ± 0.3 | |
| PCL | 85−160 | | 0 | 558 | >120 | |

[a] ± denotes standard deviation ($n$ = at least 3). Young's modulus and elongation for 44 kDa PCL were 400 MPa and 80%, respectively. Those for 50−300 kDa PLLA were 1200−3000 MPa and 2−6%, respectively.[42]

in the fluidized soft PmCL phase under the pressure with decrease in the lamellae thickness, and the resulting melt/solid mixture may flow at room temperature. On the other hand, when the applied pressure was released, the scattering profiles exactly matched those observed at the corresponding pressure during the upward pressure sweep. This indicates the reverse phase transition, from disordered to ordered state, resulting in a decrease in fluidity of the copolymer. The pressure-induced phase transition was thus completely reversible. According to the SANS results of poly(*n*-alkyl acrylate)-*b*-polystyrene by Pollard et al., pressure-induced phase mixing took place only within a few nanometers of the interface, and both phases were not completely miscible.[25] The increase in $q_{max}$ and fwhm of the scattering peak were reported, and the changes in $\Lambda_{ave}$ and its distribution were discussed. In comparison to the SANS results, the present lab-scale SAXS experiment represented less detailed information on the microphase-separated structure. However, these SAXS results were sufficient to prove the pressure-induced phase transition.

**Mechanical Properties of Degradable Block Copolymers.** Tensile testing was performed to evaluate the potential of degradable block copolyesters as alternatives to existing nondegradable thermoplastics such as polyethylene (PE). Mechanical properties of a homopolymer are primarily determined by its chemical structure, which often limits practical use. In contrast, copolymers offer an attractive solution to this limitation, and this block copolymer system is an excellent example. The results of tensile testing of various degradable block copolyesters prepared are summarized in Table 3. The stress−strain curves of some copolyesters are displayed in the Supporting Information. The Young's modulus and strain-to-break of PCL-*b*-PLLA were between those of PCL


dx.doi.org/10.1021/ma301230y | *Macromolecules* 2012, 45, 7420−7428

and PLLA homopolymers, as expected. The Young's moduli of PmCL-*b*-PLLA and PDXO-*b*-PLLA, however, were mostly lower than that of PCL, as a consequence of the amorphous nature of the soft components. In general, there are two main parameters that control the mechanical properties of the block copolymers: composition and chain length of blocks. For room-temperature processable PmCL-*b*-PLLA and PDXO-*b*-PLLA, large variations were observed in their modulus and strain-to-break even within the narrow range of block copolymer compositions studied (40−60 wt %). It was apparent that a greater hard block composition led to a higher modulus (a higher stress-at-break) and a lower strain-to-break. With PmCL-*b*-PLLA, except for the copolyester with 43 wt % LA content ($M_w$: 62 kDa) in Table 3, the increase in modulus from 62 ± 20 to 373 ± 45 MPa (increase in stress-at-break from 2.9 ± 1.0 to 6.4 ± 0.2 MPa) and the decrease in strain-to-break from 22 ± 4 to 2.0 ± 0.4% showed in nearly a linear relationship to the fraction of hard block from 47 to 60 wt %. The trends in moduli, strain-to-break, and stress-at-break with LA content seemed to be independent of the molecular weight of copolyesters. For example, PmCL-*b*-PLLA with 57 wt % LA content ($M_w$: 47 kDa) showed 441 ± 10 MPa in Young's modulus. On the other hand, the modulus of a block copolyester (LA content: 49 wt %; $M_w$: 158 kDa) was 141 ± 22 MPa. Higher LA content copolyester gave higher Young's modulus, even the molecular weight was smaller. In the case of the copolyesters with $M_w$ of 98, 20, and 48 kDa, the similar LA content resulted in the similar Young's modulus. These results indicate that each block studied was sufficiently long to entangle, forming mechanically stable virtual cross-links when the molecular weight was greater than 20 kDa. A similar tendency was found in PDXO-*b*-PLLA copolyesters. The Young's modulus increased with LA content of the block copolyester from 26 ± 2 to 459 ± 100 MPa, although relation between elongation and LA content was not clear due to a few data points. The results of these mechanical tests demonstrate that these low-temperature processable block copolyesters can be made with similar modulus to PE (800−1400 MPa for HDPE and 166−248 MPa for LDPE), although the elongation is far below.[43]

**Degradation of the Block Copolymers during Processing.** Generally, degradation of aliphatic polyesters is one of the most significant shortcomings in conventional melt-processing, limiting application and recyclability. To characterize this aspect of degradable baroplastic performance, degradation of the block copolyesters upon pressure processing was examined by SEC. The elution diagrams are displayed in the Figure 7, and the unimodal profiles also support the formation of block copolymers. In each case, SEC profiles before and after processing were identical. The molecular weight and polydispersity of each copolymer did not change by pressure processing. In addition, lower molecular weight fractions were not found after processing, indicating the chain scission is negligible during compression. This evidence shows that low-temperature processing under pressure did not cause polymer degradation. On the other hand, when PmCL-*b*-PLLA ($M_w$: 158 kDa, LA: 49 wt %) was kept at 200 °C for 30 min, the $M_w$ decreased to 121 kDa with increase in the $M_w/M_n$ from 1.8 to 2.0, which indicated thermal degradation of the copolyester upon heating.

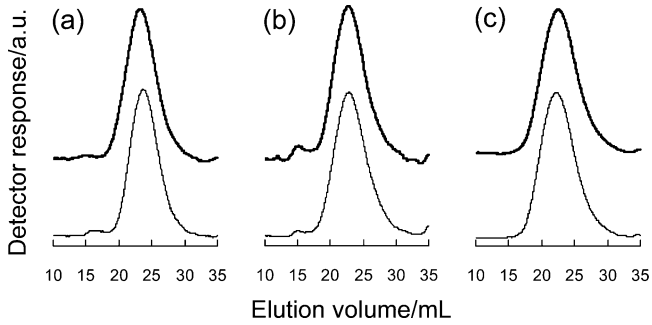


**Figure 7.** SEC diagrams of (a) PDXO-*b*-PLLA ($M_w$: 126 kDa, LA: 61 wt %), (b) PmCL-*b*-PLLA ($M_w$: 158 kDa, LA: 49 wt %), and (c) PCL-*b*-PLLA ($M_w$: 203 kDa, LA: 44 wt %) before (plain line) and after (bold line) processing.

## CONCLUSIONS

Three aliphatic block copolyesters were prepared by two-step ring-opening polymerization of the corresponding lactones and L-LA. When the composition of soft or hard segments were between 40 and 60 wt %, the block copolymers were processable at much lower temperature than the melting point of hard segment (PLLA) under 34.5 MPa. Especially, PmCL-*b*-PLLA and PDXO-*b*-PLLA could be processed at room temperature. These degradable polymers require less energy to process. The low-temperature processing also reduces polymer degradation considerably, thereby enhancing the recyclability of these polymeric materials.

The mechanism of low-temperature formability was elucidated by DSC, XRD, and SAXS. At ambient conditions, the soft and hard components of the degradable block copolymers were immiscible upon microphase separation. However, they turned to miscible under pressure and flew at the temperature. This pressure-induced phase transition observed was reversible with the polyesters developed.

## ASSOCIATED CONTENT

### Supporting Information

Thermodynamic parameters used for prediction of the phase diagram, detailed synthetic procedures of lactone monomers and block copolymers, $^1$H and $^{13}$C NMR spectra, DSC thermograms, a Hosemann's plot, a curve fitting in SAXS profile to determine the $q_{max}$ and fwhm, and stress−strain curves. This material is available free of charge via the Internet at http://pubs.acs.org.

## AUTHOR INFORMATION

### Corresponding Author

*E-mail: taniguti@rite.or.jp.

### Notes

The authors declare no competing financial interest.

## ACKNOWLEDGMENTS

This research was supported by the MIT Materials Research Science & Engineering Centers Program of the NSF under Award DMR-021282 and NIH Awards GM59870 and 5U54GM064346-03. The authors thank Prof. Anne M. Mayes and Dr. William Kuhlman for invaluable comments and discussion throughout this work. I. Taniguchi acknowledges the financial support of the Japanese Ministry of Education, Culture, Sports, Science and Technology and also thanks Prof.

Hiroshi Jinnai and Dr. Yukihiro Nishikawa for helpful discussions on the analyses of XRD.

## REFERENCES

(1) Chiellini, E.; SolaroKluwer, R. *Biodegradable Polymers and Plastics*; Kluwer Academic/Plenum Publishers: New York, 2003.
(2) Vert, M.; Feijen, J.; Albertsson, A. C.; Scott, G.; Chiellini, E. *Biodegradable Polymers and Plastics*; Royal Society of Chemistry: London, 1992.
(3) Shalaby, W. S.; Burg, J. L. K. *Absorbable and Biodegradable Polymers*; CRC Press: Boca Raton, FL, 2003.
(4) Doi, Y.; Steinbüchel, A. *Biopolymers, Polyester II-Properties and Chemical Synthesis*; Wiley-VCH: Weinheim, 2002.
(5) Doi, Y.; Steinbüchel, A. *Biopolymers, Polyester III-Applications and Commercial Products*; Wiley-VCH: Weinheim, 2002.
(6) Mercerreyes, D.; Jérôme, R.; Dubois, P. *Adv. Polym. Sci.* **1999**, *147*, 1−59.
(7) Amass, W.; Amass, A.; Tighe, B. *Polym. Int.* **1998**, *47*, 89−144.
(8) Nagata, N.; Goto, H.; Sakai, W.; Tsutsumi, N. *Polymer* **2000**, *41*, 4373−4376.
(9) Ki, H. C.; Park, O. Ok. *Polymer* **2001**, *42*, 1849−1861.
(10) Saint-Loup, R.; Jeamnarie, T.; Robin, J.-J.; Boutevin, B. *Polymer* **2003**, *44*, 3437−3449.
(11) Honda, N.; Taniguchi, I.; Miyamoto, M.; Kimura, Y. *Macromol. Biosci.* **2003**, *3*, 189−197.
(12) McNeill, I.; Leiper, H. *Polym. Degrad. Stab.* **1985**, *11*, 267−285.
(13) Jamshidi, K.; Hyon, S.-H.; Ikada, Y. *Polymer* **1988**, *29*, 2229−2234.
(14) Gonzalez-Leon, J. A.; Acar, M. H.; Ryu, S. W.; Ruzette, A. V. G.; Mayes, A. M. *Nature* **2003**, *426*, 424−428.
(15) Ruzette, A. V. G.; Mayes, A. M.; Pollard, M.; Russell, T. P.; Hammouda, B. *Macromolecules* **2003**, *36*, 3351−3356.
(16) Gonzalez-Leon, J. A.; Ryu, S. W.; Hewlett, S. A.; Ibrahim, S. H.; Mayes, A. M. *Macromolecules* **2005**, *38*, 8036−8044.
(17) Ruzette, A. V. G.; Mayes, A. M. *Macromolecules* **2001**, *34*, 1894−1907.
(18) Ruzette, A. V. G.; Banerjee, B.; Mayes, A. M.; Russell, T. P. *J. Chem. Phys.* **2001**, *114*, 8205−8209.
(19) Gonzalez-Leon, J. A.; Mayes, A. M. *Macromolecules* **2003**, *36*, 2508−2515.
(20) Matisen, T.; Masus, K.; Albertsson, A. C. *Macromolecules* **1989**, *22*, 3842−3846.
(21) Stridsberg, K.; Albertosson, A. C. *J. Polym. Sci., Part A: Polym. Chem.* **1999**, *37*, 3407−3417.
(22) Tian, D.; Dubois, P.; Grandfils, C.; Jérôme, R. *Macromolecules* **1997**, *30*, 406−409.
(23) Tian, D.; Dubois, P.; Jérôme, R. *Macromolecules* **1997**, *30*, 2575−2581.
(24) Mecerreyes, D.; Dubois, P.; Jérôme, R.; Hedrick, J. L.; Hawker, C. J. *J. Polym. Sci., Part A: Polym. Chem.* **1999**, *37*, 1923−1930.
(25) Pollard, M.; Russell, T. P.; Ruzette, A. V. G.; Mayes, A. M.; Gallot, Y. *Macromolecules* **1998**, *31*, 6493−6498.
(26) Ryu, D. Y.; Lee, D. J.; Kim, J. K.; Lavery, K. A.; Russell, T. P. *Phys. Rev. Lett.* **2003**, *90*, 235501−2355014.
(27) Taniguchi, I.; Chan, E. W. L.; Griffith, L. G.; Mayes, A. M. *Macromolecules* **2005**, *38*, 216−219.
(28) Lovell, N. G. MS. Thesis, Massachusetts Institute of Technology, 2005.
(29) Boudouris, D.; Constantinou, L.; Panayiotou, C. *Ind. Eng. Chem. Res.* **1997**, *36*, 3968−3973.
(30) van Krevelen, D. W.; Hoftyzer, P. J. *Properties of Polymers. Correlation with Chemical Structure*; Elsevier: New York, 1972.
(31) Degée, P.; Dubois, P.; Jérôme, R.; Jacobsen, S.; Fritz, H.-G. *Macromol. Symp.* **1999**, *144*, 289−302.
(32) Kricheldorf, H. R.; Kreiser-Saunders, I.; Boettcher, C. *Polymer* **1995**, *36*, 1253−1259.
(33) Witzke, D. R.; Narayan, R.; Kolstad, J. J. *Macromolecules* **1997**, *30*, 7075−7085.
(34) Möller, M.; Kånge, R.; Hedrik, J. L. *J. Polym. Sci., Part A: Polym. Chem.* **2000**, *38*, 2067−2074.
(35) Kricheldorf, H. R.; Boettcher, C.; Tönnes, K.-U. *Polymer* **1992**, *33*, 2817−2824.
(36) Andronova, N.; Finne, A.; Albertsson, A.-C. *J. Polym. Sci., Part A: Polym. Chem.* **2003**, *41*, 2412−2423.
(37) Tsuji, H.; Suzuyoshi, K. *Polym. Degrad. Stab.* **2002**, *75*, 347−355.
(38) Hosemann, R.; Wilke, W. *Makromol. Chem.* **1968**, *118*, 230−249.
(39) Brizzolara, D.; Cantow, H.-J.; Diederichs, K.; Keller, E.; Domb, A. J. *Macromolecules* **1996**, *29*, 191−197.
(40) Kobayashi, J.; Asahi, T.; Ichiki, M.; Oikawa, A.; Suzuki, H.; Watanabe, T.; Fukuda, E.; Shikinami, Y. *J. Appl. Phys.* **1995**, *77*, 2957−2973.
(41) Matsen, M. W.; Bates, F. S. *Macromolecules* **1996**, *29*, 7641−7644.
(42) Cristina, M.; Martins, L. In *Biomaterials Science*, 2nd ed.; Ratner, B. D., Hoffman, A. S., Schoen, F. J., Lemons, J. E., Eds.; Elsevier: Boston, 2004; pp 819−821.
(43) DeLassus, P. T.; Whiteman, N. F. In *Polymer Handbook*, 4th ed.; Brandrup, J., Immergut, E. H., Grulke, E. A., Abe, A., Bloch, D. R., Eds.; Wiley-Interscience: New York, 1998; Vol. *1*, pp V/159−169.